



SCAN-9601225

509606

RECENT STUDIES ON TOP QUARK PHYSICS AT NLC <sup>a</sup>P. Comas<sup>1</sup>, M. Martínez<sup>2</sup>, R. Miquel<sup>1</sup>, S. Orteu<sup>2</sup> and M. Schmitt<sup>3,b</sup><sup>1) CERN, CH-1211 Geneva 23, Switzerland</sup><sup>2) Institut de Física d'Altes Energies, Universitat Autònoma de Barcelona  
E-08193 Bellaterra (Barcelona), Spain</sup><sup>3) Department of Physics, University of Wisconsin  
Madison, WI53706, USA</sup>

## Abstract

Recent studies done by the "European Experimental Working Group on Top Quark Physics at the NLC", are briefly summarized. The studies concern three topics: threshold scan, measurement of the top Yukawa coupling and measurement of the top production and decay form factors.

## 1 Introduction

After several studies during the last ten years on the physics potential of a high energy linear  $e^+e^-$  collider (NLC) and its actual feasibility (see for instance references<sup>1,2</sup>), such a facility is emerging as a realistic complementary programme to the LHC effort. A linear  $e^+e^-$  collider with centre-of-mass energies in the range 350-1000 GeV has been shown to have an wide physics programme among which one of the most important topics is the detailed study of the properties of top quarks.

Top quarks will be copiously pair-produced at such a machine and, since they are heavier than the intermediate vector bosons, and maybe even heavier than the Higgs boson, it is not unreasonable to think that their properties might well be different from the ones of the lighter quarks and that they can shed some light over the mechanism of mass generation and provide valuable information for the understanding of flavour symmetries.

The dominant top production channel goes through the  $e^+e^-$  annihilation to a virtual photon or  $Z$ , which subsequently will decay to a  $t\bar{t}$  pair. The  $t\bar{t}$  production cross section is about 650 fb at  $\sqrt{s} = 500$  GeV. At the foreseen luminosities of  $10^{33} - 10^{34} \text{ cm}^{-2} \text{ s}^{-1}$  (or  $10 - 100 \text{ fb}^{-1}$  per year) the event sample is sufficient for detailed studies.

In the Minimal Standard Model (MSM) the top decays essentially 100% of the times into a bottom quark and a  $W$ . Depending on the decays of the two  $W$ 's present in the event, the  $t\bar{t}$  event will consist of six jets (44%); four jets, a high-momentum lepton and a neutrino (44%);

or two jets, two high-momentum leptons and two neutrinos (11%). In all cases there will be two  $b$  jets. The total top quark width is given approximately by  $\Gamma_t \sim 0.18 \text{ GeV}(m_t/M_W)^3$ , which is about 2 GeV for  $m_t = 180 \text{ GeV}$ .

The following topics in top quark physics will be discussed here: i) the measurements of the top quark mass and width in a centre-of-mass energy scan around threshold, ii) the possible direct determination of the  $t\bar{t}H$  Yukawa coupling and iii) the determination of the top production and decay form-factors.

## 2 Threshold scan studies

The large decay rate of the top quark implies that it decays before the toponia bound states have had time to form. More generally,  $\Gamma_t$  acts as an effective cut-off energy for non-perturbative QCD effects. This makes easier the studies and the predictions, in particular, near the  $t\bar{t}$  production threshold.

An energy scan around the  $t\bar{t}$  threshold can be used to do a precise measurement of the top quark mass. Three observables are available:

- The total production cross section,  $\sigma_{t\bar{t}}(s)$ , is particularly sensitive to  $m_t$ . However, it is also quite sensitive to the strength of the  $t\bar{t}$  binding potential.
- The top momentum distribution,  $d\sigma/dp(s)$ , depends also on the top mass and the potential.
- The forward-backward asymmetry,  $A_{FB}(s)$ , due to the interference of S- and P-wave amplitudes, provides a third handle on the top mass.

Theoretical calculations for these three quantities are available<sup>3,4</sup>. They are based on the computation of the non-relativistic Green's function<sup>5</sup>

$$\tilde{G}(p; E; m_t, \alpha_s, \Gamma_t) \equiv (p|G|r=0),$$

where  $p$  is the top quark momentum and  $E \equiv \sqrt{s} - 2m_t$ .  $G$  verifies the Schrödinger equation

$$(H - E - i\Gamma_t)G = 1,$$

$H$  being the Hamiltonian, which includes the QCD potential. The three observables described above can be obtained directly from  $G$  or its Fourier transform,  $\tilde{G}$ .

The shape of the threshold is distorted by initial state radiation effects as well as by energy smearing due to the accelerator (fig. 1). The last effect is particularly important and leads to a substantially less steep threshold and a considerable reduction in the cross section. Both effects

<sup>a</sup>Presented by M. Martínez at the "Workshop on Physics and Experiments with Linear Colliders", September 8-12, Morioka-Appi, Iwate, Japan

<sup>b</sup>Supported by the US Department of Energy, grant number DE-FG0295ER40896.

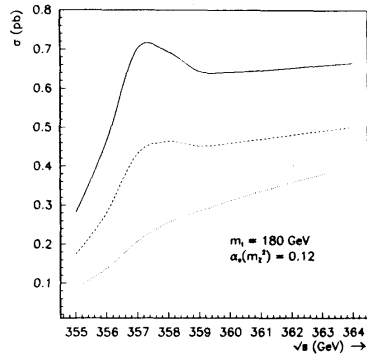


Figure 1:  $t\bar{t}$  production cross section as a function of the centre-of-mass energy. Solid line: Born cross section; dashed line: with initial state radiation (ISR); dotted line: with ISR and beam effects, computed with the parameters of the TESLA accelerator design<sup>6</sup>.

decrease substantially the sensitivity of the cross section measurement to the top mass. The top momentum distribution and the forward-backward asymmetry are also affected, although at a smaller level.

The cross section measurement uses events with six or five jets, one of which can consist of just a lepton. By asking that the event be spherical and using the two  $W$  mass constraints and the two top quark mass constraints, a sample of  $t\bar{t}$  events can be selected with 33% overall efficiency and signal to background ratio in excess of five.<sup>1</sup>

For the measurements of  $d\sigma/dp$  and  $A_{FB}$  only events in which one  $W$  decays leptonically are used. This way, the charge of one of the tops is readily obtained from the lepton charge while the other top is used to measure the momentum. Backgrounds have been found to be negligibly small and the overall efficiency close to 15%<sup>2</sup>. The resolution in the top momentum is about 10%. The position of the maximum of the top momentum distribution can be obtained with a 3 GeV error with a luminosity of  $5 \text{ fb}^{-1}$ . The probability of charge confusion, relevant for

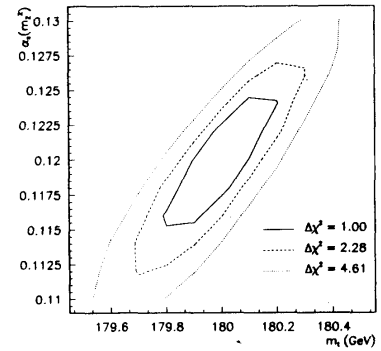


Figure 2: Results of the  $\chi^2$  fit using the total cross section, momentum distribution and forward-backward charge asymmetry.

$A_{FB}$ , has been found to be at the level of few per cent.

The total cross section, position of peak of the momentum distribution and forward-backward asymmetry, all as a function of centre-of-mass energy, are the observables chosen to extract the top mass. The peak of the momentum distribution was chosen because it was found<sup>2</sup> to be rather insensitive to beam effects. The three observables are used in a  $\chi^2$  fit assuming a nine-point scan around  $\sqrt{s} = 360 \text{ GeV}$  with an integrated luminosity of  $5 \text{ fb}^{-1}$  in each point. Another  $5 \text{ fb}^{-1}$  are assumed to be taken below the threshold in order to measure the background.

The fit has two free parameters: the top quark mass and  $\alpha_s$ , which appears in the QCD  $t\bar{t}$  potential. The resulting two-dimensional  $\chi^2$  contours can be seen in fig. 2. The overall precision expected in the top quark mass is around 200 MeV. The strong coupling constant at the  $Z$  scale is determined with a  $\pm 0.005$  uncertainty. Most of the sensitivity comes from the total cross section measurement, with a non-negligible improvement coming from  $d\sigma/dp$ . The forward-backward asymmetry does not contribute significantly to the final result.

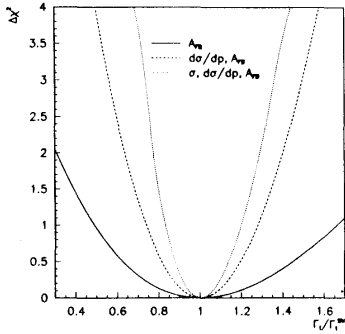


Figure 3:  $\chi^2$  increase as a function of the top width using only the forward-backward charge asymmetry (solid line), adding the top momentum information (dashed line) and adding as well the total cross section information (dotted line).

The extra degree of freedom represented by  $\alpha_s$  can actually be viewed as a way to parametrize uncertainties in the binding QCD potential. For instance, in the scale at which the strong coupling constant has to be evaluated, or in the exact form of the long-distance part of the potential, although this has a limited impact due to the large top width.

The same data and observables can also be used to determine the top quark width. The forward-backward asymmetry is expected to be quite sensitive to the width. Since its origin lies in the interference of the S- and P-wave amplitudes, a larger width implies more overlap between the two resonances and, therefore, larger asymmetry. The increase in  $\chi^2$  when performing a fit similar to the one described above (nine energy points with  $5 \text{ fb}^{-1}$  each) with only  $\Gamma_t$  free is shown in fig. 3. The sensitivity of the asymmetry exists but it is rather modest. Including the three observables, the overall precision in the top quark total width will be around 18%, for fixed values of  $m_t$  and  $\alpha_s$ .

### 3 Top Yukawa coupling

Even if the MSM Higgs is found, the coupling to the other fundamental particles must be measured to check the Higgs mechanism. Since the Higgs coupling to fermions is proportional to the fermion mass squared,  $\lambda_f^2 = (m_f/v)^2$  being  $v = (\sqrt{2}G_F)^{1/2} \simeq 246 \text{ GeV}$ , the Yukawa coupling for the top quark is much larger than for any other fermion:  $\lambda_t^2 \sim 0.5$  whereas, for instance  $\lambda_b^2 \sim 0.0004$ . Therefore, the top quark provides a unique opportunity to measure the Yukawa coupling.

The top Yukawa coupling might show its effects in several observables. It has some effect, for instance, in the interquark potential near the top production threshold and hence, indirectly affects the threshold observables discussed in the previous section. Rather than these sort of measurements, in this section we wanted to concentrate in the feasibility of a more direct measurement of this coupling.

For the direct measurement of the top Yukawa coupling, two different scenarios should be distinguished:

(1) "Heavy Higgs" ( $M_H > 2m_t$ ). In this case, the fermionic Higgs decays would predominantly be into  $t\bar{t}$ , which would compete with the bosonic Higgs decays. The Higgs could predominantly be produced either through the "standard" Bjorken mechanism  $e^+e^- \rightarrow ZH$  or through the  $W$  fusion mechanism in  $e^+e^- \rightarrow \nu\nu H$  (see fig. 4) and afterwards decay into  $t\bar{t}$ . These processes constitute the basic mechanism for Higgs searches and hence, have already been studied in that context by several authors.

(2) "Light Higgs" ( $M_H < 2m_t$ ). In this case, the fermionic Higgs decays would predominantly be into  $b\bar{b}$ . If the Higgs is heavier than twice the  $W$  or the  $Z$  mass they would compete with the bosonic decays. The Higgs could be produced through "radiation" off a top ("Higgs-strahlung", see fig. 4). Since the detectability of this process had not been studied, that is the process that we want to discuss in detail.

#### 3.1 Theoretical aspects

The calculation for the "Higgs-strahlung" with only  $\gamma$ -exchange existed since long time ago<sup>7</sup> and few years ago the complete calculation was also finished<sup>8</sup>. Since at the NLC energies the  $\gamma$ -exchange contribution dominates by far, both calculations are in good agreement.

The total cross section, for any given value of  $M_H$  decreases at low  $\sqrt{s}$  due to phase space and also decreases at high  $\sqrt{s}$  due to unitarity. For the range of  $M_H < 2m_t$ , the cross section is maximal around 750 GeV but reaches only  $O(1-10 \text{ fb})$  as can be gleaned from fig. 5.

Assuming "ideal" detection conditions (100% acceptance and 0% background) figure 6 shows for three different  $\sqrt{s}$  the sensitivity  $S$  to

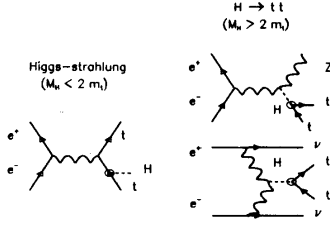


Figure 4: Feynman diagrams for the processes that can be used to directly measure the top Yukawa coupling.

$\lambda_t^2$  as a function of the Higgs mass, defined in such a way that

$$\Delta\lambda_t^2 = \frac{1}{S\sqrt{L}} \quad (1)$$

where  $L$  stands for the luminosity in  $\text{fb}^{-1}$ . Therefore, ideally one could make a measurement at the level of  $\Delta\lambda_t/\lambda_t \sim 0.1$  with  $50 \text{ fb}^{-1}$  for  $M_H < 240 \text{ GeV}$ .

### 3.2 Experimental aspects

Using the calculation by Djouadi et al. <sup>8</sup> we have written a complete M.C. event generator to make an experimental simulation of this process. The events have been processed with PYTHIA and smeared to simulate "standard detector" conditions <sup>1</sup>.

Assuming that the Higgs decays with a 100% branching ratio into  $b\bar{b}$  (which is a good approximation for  $M_H < 160 \text{ GeV}$ ) the signal consists in  $e^+e^- \rightarrow t\bar{t}H \rightarrow W^+bW^-\bar{b}b\bar{b}$ . By taking only hadronic  $W$  decays, then we have  $jjb\bar{b}jj\bar{b}\bar{b}$  so that the basic signature consists in a 8 jet event which has 4  $b$  plus 4 non- $b$  jets which can be selected using  $b$ -tagging plus  $2 M_W$ ,  $2 m_t$  and the  $M_H$  constraints. The analysis of the 6 jet plus lepton and 4 jet plus 2 lepton configurations has not yet been carried out. We have simulated specifically the case in which  $M_H = 100 \text{ GeV}$  and our selection procedure had the following steps:

7

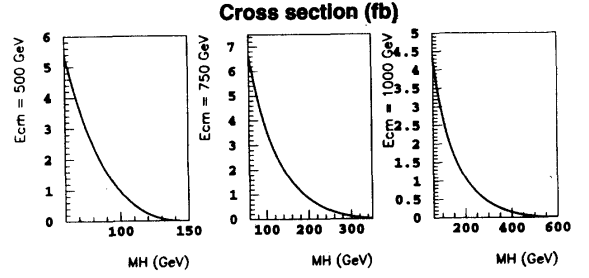


Figure 5: Total cross section for the "Higgs-strahlung" process as a function of  $M_H$  for different  $E_{cm}$ .

- Require  $> 7$  jets but force the event afterwards to have 8 jets
- Discard events with jets being just one lepton
- Apply  $b$ -tagging to the jets to classify them into  $b$  and non- $b$  jets. In this step we have assumed that  $b$  hadrons can be identified with very high efficiency (we take 100%) and a jet is assumed to be a  $b$  jet if, at least, half of its energy comes from  $b$  hadrons. Therefore the actual  $b$  tagging efficiency that we assume is not 100% but it is still very high.
- Find best  $W$ -mass combination for non- $b$  jets.
- Find best  $H$ -mass combination for  $b$  jets and require  $80 \text{ GeV} < M_H < 110 \text{ GeV}$ .

Figure 7 shows the invariant mass distributions obtained.

Concerning backgrounds, there are, for the signature that we have chosen to identify our signal, at least two potentially dangerous channels:

- (1)  $e^+e^- \rightarrow t\bar{t}Z$ . The cross section is similar to the one of the signal but the requirement of  $Z \rightarrow b\bar{b}$  introduces an additional factor 10 decrease. The Higgs invariant mass cut could reduce in addition the background if the Higgs mass is sensibly different from the  $Z$  mass, which is not the case for  $M_H = 100 \text{ GeV}$ , our choice for the simulation. In our case, the signature of this process is irreducibly mixed with the one of the

8

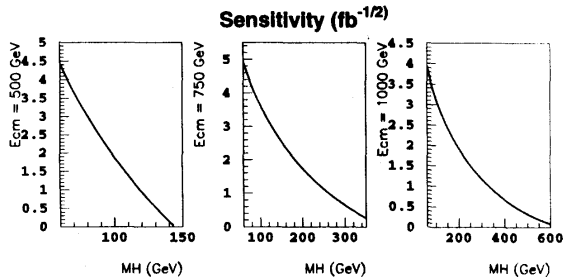


Figure 6: Ideal sensitivity function  $S$  to  $\lambda_2^2$  as a function of  $M_H$  for different  $E_{cm}$  (see text for the precise definition).

signal and hence, we have not directly simulated it but rather considered that it would contribute unavoidably to about 10% of the signal.

(2)  $e^+e^- \rightarrow t\bar{t}$  where, due to confusion in the jet assignment or due to the actual production of additional  $b\bar{b}$  pairs (for instance coming from virtual gluon emission) the signal signature is emulated. In spite of the a priori low probability of such a background, the fact is that, since the cross section for  $e^+e^- \rightarrow t\bar{t}$  is of about two orders of magnitude larger than the one for the signal, some background might still be expected. We have simulated this process by using JETSET.

The preliminary results of the selection for the signal and the background are shown in table 1. As can be seen in that table, even assuming a 100% b-meson tagging efficiency, the total selection efficiency is smaller than 30 % and the signal to noise ratio is below 2. Therefore, our preliminary conclusion, is that the measurement seems to be at the limit of being possible and, in any case, it is clear that a detailed simulation of the b-tagging is crucial to make a quantitative statement about the actual sensitivity that can be obtained in the measurement of the top Yukawa coupling.

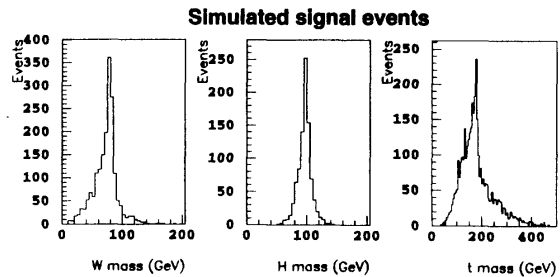


Figure 7: Reconstructed invariant mass distributions for the "Higgs-strahlung" signal events. In the top mass distribution, the combinatorial background is also shown.

#### 4 Production and Decay Form Factors

The production and decay of top quarks at a future linear collider provides opportunities to detect physics beyond the MSM. There can be anomalous form factors associated to the production vertex which modify the  $t\bar{t}$  coupling to the neutral electroweak current, and to the decay vertex which modify coupling to the weak charged current. The presence of such anomalous couplings, if large enough, would be observed in the angular and energy distributions of the  $t\bar{t}$  final state.

Top quarks are produced in  $e^+e^-$  collisions with a high longitudinal polarization. In contrast to lighter quarks, this polarization is not obscured during hadronization because the top quark decays too quickly. Consequently, the initial top helicity is transferred efficiently to the final state.

The current operator can be written

$$j_\mu^a \propto \gamma_\mu (F_{1L}^a P_L + F_{1R}^a P_R) + \frac{i\sigma_{\mu\nu} q^\nu}{2m_t} (F_{2L}^a P_L + F_{2R}^a P_R), \quad (2)$$

where  $F^a$  are form factors. In the MSM,  $F_{1L}^a = F_{1R}^a = F_{1L}^W = 1$ ,  $F_{1R}^Z = g_L$ ,  $F_{1R}^W = g_R$ , and  $F_{2L}^a = F_{2R}^a = F_{2L}^W = 0$ . A nonzero value for  $F_{2L}^a + F_{2R}^a$  would be caused by a magnetic quadrupole moment, and nonzero

Table 1: Results of the experimental simulation for the Yukawa coupling measurement assuming an integrated luminosity of  $50 \text{ fb}^{-1}$

Energy (GeV)	500	750	1000
$t\bar{t}$ (signal)			
x-section (fb)	.95	3.6	2.8
Events ( $50 \text{ fb}^{-1}$ )	13.1	47.5	22.6
$t\bar{t}$ (background)			
x-section (fb)	550	300	175
Events ( $50 \text{ fb}^{-1}$ )	11.0	28.5	28.0
Signal/noise	1.2	1.7	1.3

value for  $F_{2L}^{\gamma,Z} - F_{2R}^{\gamma,Z}$  by a weak electric dipole moment. These would influence the production distributions for top quarks. If  $F_{1R}^W \neq 0$ , then there might be a  $V + A$  admixture to the top charged current, or a  $W_R$  boson.  $F_{1R}^W$  is tested in the study of decay distributions of top quarks.

We have performed simple investigations of the production and decay distributions to estimate the statistical precision attainable at a future linear collider. The results are presented in the next two sections.

#### 4.1 Production Vertex

The polar angle distribution of the  $t\bar{t}$  pair contains, in addition to the usual  $1 + \cos^2 \theta$  terms, a term proportional to  $\sin^2 \theta$ :

$$\frac{d\sigma}{d\cos\theta} \propto \sin^2 \theta \cdot \left[ \frac{m_t}{E} (F_{1L} + F_{1R}) + \frac{E}{m_t} 2(F_{2L} + F_{2R}) \right]^2. \quad (3)$$

The normal spin-flip probability, proportional to  $1/\gamma^2$ , is augmented by an anomalous term which grows with energy<sup>9,10</sup>.

The extra piece ( $F_{2L} + F_{2R}$  in Eq. 3) increases the total cross section as well as changes the differential distribution. In order to extract information which was not already included in the cross section measurement, we chose to perform a maximum likelihood fit to the polar angle distribution to detect an anomalous  $\sin^2 \theta$  piece:

$$\mathcal{P}_{\text{obs}} = (1 - \delta) \cdot \mathcal{P}_{\text{SM}} + \delta \cdot \mathcal{P}_{\text{anom}} \quad (4)$$

where  $\delta$  is a single free parameter. (It is not the same symbol  $\delta$  as used in Ref. 9,10.) The probability density for the MSM is assumed known (see for example Ref. 11); the anomalous piece is simply  $\frac{4}{3} \sin^2 \theta$ . A value for  $\delta$  significantly greater than zero signals new physics.

case	$\Delta\delta$
ideal	0.015
selection efficiency	0.026
acceptance (as function of $\theta$ )	0.033
resolution	0.034
flip (15% probability)	0.038
backgrounds (20% contamination)	0.041

Table 2: Statistical sensitivity to an anomalous  $\sin^2 \theta$  term in the production cross section, as realistic effects are included in a toy Monte Carlo simulation.  $m_t = 180 \text{ GeV}$ ,  $\sqrt{s} = 500 \text{ GeV}$ ,  $\mathcal{L} = 50 \text{ fb}^{-1}$ .

Samples generated with a toy Monte Carlo program were fit to expression 4, and the distribution of  $\delta$  examined to determine the statistical uncertainty. The toy program was tuned to approximate a full simulation for  $m_t = 180 \text{ GeV}$  and  $\sqrt{s} = 500 \text{ GeV}$ . At this energy the boost of the top quarks is sufficient to allow a reasonably precise measurement of their direction. It is not necessarily the most optimal energy for this measurement.

The top quark direction is taken to be the thrust axis of the event. An energetic, isolated electron or muon is needed to sign the angle. Simulations with PYTHIA give the efficiency of the selection, the resolution on the top direction, the acceptance as a function of polar angle, probability to mis-sign the angle (the 'flip probability'), and the non-top contamination. Detector performance was approximately that of the Aleph detector. All of these effects are incorporated in the toy program. An illustration of the reconstructed polar angle distribution is shown in Figure 8. The clear asymmetry from the top quark is evident despite the contamination, dominated by  $W$  pairs and  $b\bar{b}$ , which peaks in the opposite direction.

The statistical sensitivity is given in Table 2, showing how it decreases as each realistic effect is included. Ultimately, the statistical error would be about  $\Delta\delta = 0.04$ , for an integrated luminosity of  $50 \text{ fb}^{-1}$ .

#### 4.2 Decay Vertex

The charged weak current in the MSM is pure  $V - A$ , leading to unambiguous predictions for the energy and angular decay distributions of leptons. A small admixture of  $V + A$  interaction modifies these distributions; the difference between pure  $V + A$  and pure  $V - A$  is large for neutrinos in decays of down-type fermions, and for leptons in up-type fermions. The L3 Collaboration has used this difference to constrain the charged current in  $b$  decays<sup>12</sup>.

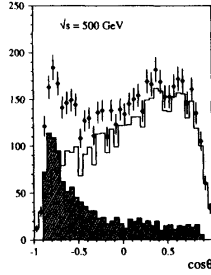


Figure 8: Simulated thrust axis polar angle distribution, signed by an energetic, isolated lepton. The contributions of  $t\bar{t}$  and background are shown separately.  $m_t = 180$  GeV and  $\sqrt{s} = 500$  GeV.

The theoretical work has been carried out by Jezabek and others<sup>13</sup>; the decay distributions are known including first order QCD corrections. They can be written in terms of a parameter  $\kappa$ , such that  $g_V = (1 + \kappa)/\sqrt{1 + \kappa^2}$  and  $g_A = (-1 + \kappa)/\sqrt{1 + \kappa^2}$ , so  $\kappa^2 = 0$  is the MSM and  $\kappa^2 \rightarrow \infty$  is pure  $V + A$ . (See Ref.<sup>13</sup> for complete expressions.) The experimental task is to constrain  $\kappa^2$  using as much information as possible from the lepton energy and direction, and if possible, from the neutrino.

These studies were performed using top decays simulated at threshold, since in this case the top spin points along the beam direction, and the energy and angle of the lepton in the lab frame are essentially the same as those in the top rest frame. An integrated luminosity of  $100 \text{ fb}^{-1}$  was assumed.

The lepton energy and angular resolution is good enough so as to have little impact on the measurement. The neutrino measurement is less certain, due to unknown and variable losses to ISR, and detector acceptance. Nonetheless, a resolution of about 10% was obtained from the simulation. The energy and angular distributions for the lepton were condensed into a single "optimal" variable  $\omega_l$ , and for the neutrino, a separate variable  $\omega_\nu$ . The mean  $\omega$  changes monotonically as a function of

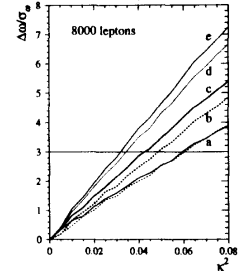


Figure 9: Increase in significance  $\Delta\omega/\sigma_\omega$  as  $\kappa^2$  is increased. The inclusion of more information results in a steeper line: a) lepton or neutrino energy alone, b) neutrino energy and angle, c) lepton energy and angle, d) lepton energy and angle, and neutrino energy, e) lepton and neutrino energies and angles.

$\kappa^2$ ; the significance of a shift in terms of the variance of  $\omega$  is the statistical sensitivity of a measurement. This significance ( $\Delta\omega/\sigma_\omega$ ) is plotted as a function of  $\kappa^2$  in Figure 9. The increase in sensitivity as more information is taken into account is manifested as a steeper line; the shift passes three sigma for a twice smaller value of  $\kappa^2$  when all information from the lepton and neutrino are used compared to the lepton energy alone. (A single optimized variable incorporating the lepton and neutrino information was not constructed explicitly; rather, the significances for the lepton and the neutrino were added together in quadrature.) Resolution and acceptance degrade the sensitivity by about 20%. The ultimate statistical uncertainty would be approximately  $\Delta\kappa^2 \approx 0.013$  for an integrated luminosity of  $100 \text{ fb}^{-1}$ , at threshold.

#### Acknowledgments

We thank M. Chmeissani for his help in the early stages of this work. We are indebted to M. Jezabek and his collaborators for providing us their computer programs for several of the studies discussed here, as well

as for many discussions. Two of us (M. M. and R. M. ) would also like to thank the organizers for the warm hospitality and the perfect organization of the workshop.

#### References

1. G. Bagliesi et al. in *Proceedings of the Workshop on  $e^+e^-$  Collisions at 500 GeV: The Physics Potential (Munich, Annecy, Hamburg, February 1992-September 1992)*, ed. P. M. Zerwas, DESY report 92-123A, pp. 327-377.
2. P. Igo-Kemenes, M. Martinez, R. Miquel and S. Orteu in *Proceedings of the 1993 Workshop on  $e^+e^-$  Physics at 500 GeV: The Physics Potential (Munich, Annecy, Hamburg, November 1992-April 1993)*, ed. P. M. Zerwas, DESY report 93-123C, pp. 319-329.
3. M. Jezabek, J. H. Kühn and T. Teubner, *Z. Phys. C* 56 (1992) 653; M. Jezabek and T. Teubner, *Z. Phys. C* 59 (1993) 669; R. Harlander, M. Jezabek, J. H. Kühn and T. Teubner, *Phys. Lett.* B346 (1995) 137.
4. Y. Sumino et al., *Phys. Rev. D* 47 (1992) 56.  
See also M. J. Strassler and M. E. Peskin, *Phys. Rev. D* 43 (1991) 1500.
5. V. S. Fadin and V. A. Khoze, *Sov. J. Nucl. Phys.* 48 (1988) 309.
6. D. Schulte, private communication.
7. K. J. F. Gaemers and G. J. Gounaris, *Phys. Lett.* 77B (1978) 379.
8. A. Djouadi, J. Kalinowski and P. M. Zerwas, *Z. Phys.* C54 (1992) 255.
9. M. Peskin, proceedings of the Linear Collider workshop held in Saariselkä, Finland, 9-14. Sept. 1991, pp. 1-50.
10. C. Schmidt, SCIPP 95/14, hep-ph/9504434.
11. M. Jezabek, *Nucl. Phys. B (Proc. Suppl.)* 37B (1994) 197.
12. L3 Collaboration, *Phys. Lett. B* 351 (1995) 375.
13. M. Jezabek, TTP 95-12 (March, 1995)  
M. Jezabek and J.H. Kühn, *Phys. Lett.* B329 (1994) 317.  
M. Jezabek and J.H. Kühn, *Nucl. Phys.* B320 (1989) 20.